



Published in final edited form as:

Exp Physiol. 2019 March ; 104(3): 334–344. doi:10.1113/EP087445.

¹²⁵Iodide as a surrogate tracer for epithelial chloride transport by the mouse large intestine *in vitro*.

Christine E. Stephens, Jonathan M. Whittamore, and Marguerite Hatch

Department of Pathology, Immunology, and Laboratory Medicine, College of Medicine, University of Florida, Gainesville, FL

Abstract

Chloride (Cl⁻) transport is important for driving fluid secretion and absorption by the large intestine with dysregulation resulting in diarrhea-associated pathologies. The radioisotope ³⁶Cl⁻ has long been used as a tracer to measure epithelial Cl⁻ transport but is prohibitively expensive. ¹²⁵Iodide has been used as an alternative to ³⁶Cl⁻ in some transport assays but has never before been validated as an alternative for tracing bidirectional transepithelial Cl⁻ fluxes. This study's goal was to validate ¹²⁵I⁻ as an alternative to ³⁶Cl⁻ for measuring Cl⁻ transport by the intestine. Simultaneous fluxes of ³⁶Cl⁻ and ¹²⁵I⁻ were measured across the mouse cecum and distal colon. Net Cl⁻ secretion was induced by the stimulation of cAMP with a cocktail of forskolin (FSK) and 3-isobutyl-1-methylxanthine (IBMX). Unidirectional fluxes of ¹²⁵I⁻ correlated well with ³⁶Cl⁻ fluxes following cAMP-induced net Cl⁻ secretion, occurring predominantly through a reduction in the absorptive mucosal-to-serosal Cl⁻ flux rather than stimulation of the secretory serosal-to-mucosal Cl⁻ flux. Correlations between ¹²⁵I⁻ fluxes and ³⁶Cl⁻ fluxes were maintained in epithelia from mice lacking DRA (Slc26a3), the main Cl⁻/HCO₃⁻ exchanger responsible for Cl⁻ absorption by the large intestine. Lower rates of Cl⁻ and I⁻ absorption in the DRA KO intestine suggest that DRA may have a previously unrecognized role in iodide I⁻ uptake. This novel study validates ¹²⁵I⁻ traces transepithelial Cl⁻ fluxes across the mouse large intestine, provides insights into the mechanism of net Cl⁻ secretion and suggests DRA may be involved in intestinal iodide absorption.

Keywords

chloride transport; iodide transport; tracer; intestine; Slc26a3; cAMP

Address for correspondence: C. E. Stephens, Department of Pathology, Immunology, and Laboratory Medicine, College of Medicine, University of Florida, PO box 100275, 1600 SW Archer Rd, Gainesville, FL 32610, U.S.A. stephenc@ufl.edu, Tel: (352) 273 8116, Fax: (352) 392 3053.

Author contribution

J.M.W. and M.H. conceived research; C.E.S., J.M.W. and M.H. designed research; C.E.S. performed experiments; C.E.S. and J.M.W. analyzed data; C.E.S., J.M.W. and M.H. interpreted experimental result; C.E.S. prepared figures; C.E.S. drafted manuscript; C.E.S., J.M.W. and M.H. edited and revised manuscript; C.E.S., J.M.W. and M.H. approved final version of the manuscript and agree to be accountable for all aspects of the work in ensuring that the questions related to the accuracy or integrity of any part of the work are appropriately investigated and resolved. All persons designated as authors qualify for authorship, and all those who qualify for authorship are listed.

Competing interests

The authors have no conflicts of interest, financial or otherwise, to declare.

Introduction

The isotope $^{36}\text{Cl}^-$ has been used as a radioactive tracer of chloride for many decades, contributing significantly to our understanding of Cl^- transport across the intestinal epithelium (Bridges, Rummel, & Simon, 1983; Curran, 1960; Field, 1971; Freel, Whittamore, & Hatch, 2013; M Hatch, Freel, & Vaziri, 1994; Marguerite Hatch, Freel, & Vaziri, 1993; Nobles, Diener, & Rummel, 1991; Seidler et al., 2008; J. Walker, Jijon, Churchill, Kulka, & Madsen, 2003; Yajima, Suzuki, & Suzuki, 1988). However, in recent years, the use of ^{36}Cl has become unfeasible due to its scarcity and cost. For example, in the past 15 years the price of ^{36}Cl has sky-rocketed almost 70-fold and now costs over \$100 per μCi compared to just \$1.50 per μCi in 2003.

As an alternative, short circuit current (I_{sc}) has become a popular surrogate of net electrogenic Cl^- secretion across cultured cell monolayers and native epithelia (Clarke, 2009; Li, Sheppard, & Hug, 2004; Moran & Zegarra-Moran, 2008). However, I_{sc} is a composite of the major ions (i.e. Na^+ , HCO_3^- , Cl^- and K^+) which also contribute to this metric thus making it difficult to distinguish Cl^- . Additionally, electroneutral Cl^- transport, for example $\text{Cl}^-/\text{HCO}_3^-$ exchange and Na^+-Cl^- cotransport, will not be represented by I_{sc} . The recent generation of knockout (KO) mouse models lacking various intestinal Cl^- transporters (Flagella et al., 1999; Gawenis et al., 2004; Oppermann et al., 2007; Schweinfest et al., 2006; Wang et al., 2005) provide a valuable opportunity to parse the contribution of individual transporters to epithelial Cl^- transport. However, the cost of $^{36}\text{Cl}^-$ is clearly unsustainable and thus threatens to limit future studies of this important anion leading us to consider alternatives for measuring transepithelial Cl^- transport.

One approach would be to use an alternative tracer for Cl^- , in much the same way $^{86}\text{Rb}^+$ serves as a surrogate for K^+ transport (Cheval & Doucet, 1990; M Hatch, Freel, & Vaziri, 1998; Ribeiro, Heinke, & Diener, 2001; Venglarik, Bridges, & Frizzell, 1990). In terms of Cl^- , $^{125}\text{I}^-$ was previously shown to be a suitable surrogate for ^{36}Cl to measure Cl^- efflux from cultured cells (Venglarik et al., 1990). Indeed, one of the advantages of using $^{125}\text{I}^-$ noted by Venglarik et al. (1990) was the cost differential where, at the time, $^{125}\text{I}^-$ was merely “1/10 that of ^{36}Cl ”. This price gap has greatly expanded and $^{125}\text{I}^-$ is now more than 1/500th the cost of ^{36}Cl . More recently, $^{125}\text{I}^-$ has been used to measure $\text{Cl}^-/\text{HCO}_3^-$ exchange activity and Cl^- absorption by cultured Caco-2 cells (Gujral et al., 2015; Kravtsov et al., 2016; Kumar et al., 2014) and everted gut sacs of mouse large intestine (Saksena et al., 2010) respectively. However, neither reported a direct comparison of I^- with Cl^- and, although the latter was the first instance in which ^{125}I was used to examine Cl^- transport by epithelia, it only presented a single unidirectional flux. $^{125}\text{I}^-$ has, to the best of our knowledge, never been investigated as a suitable alternative to $^{36}\text{Cl}^-$ for studying bidirectional Cl^- transport pathways across an intact, heterogeneous epithelium. Additionally, by adopting the Ussing chamber technique we can also simultaneously record and match Cl^- and I^- fluxes to I_{sc} , a popular surrogate of net Cl^- secretion.

The goal of this study was to evaluate ^{125}I as an alternative to ^{36}Cl for the measurement of unidirectional Cl^- fluxes across the intact epithelium of the large intestine using Ussing chambers. Using the mouse model, we simultaneously measured ^{125}I and ^{36}Cl transport by

the intact large intestine and their respective responses to cAMP-stimulated anion secretion. Additionally, we examined the impact of the $\text{Cl}^-/\text{HCO}_3^-$ exchanger DRA (Down-Regulated in Adenoma; Slc26a3), one of the main Cl^- transporters in the large intestine (Alper et al., 2011; Freel et al., 2013; Schweinfest et al., 2006; Whittamore, Freel, & Hatch, 2013), prominently expressed in the cecum and distal colon (Talbot & Lytle, 2010), on Cl^- and I^- fluxes with and without cAMP stimulation.

Materials and methods

Ethical approval

All experimental procedures were approved by the University of Florida Institutional Animal Care and Use Committee (IACUC) in accordance with the National Institutes of Health *Guide for the Care and Use of Laboratory Animals* (protocol approval number 201803127). All experimental procedures comply with *Experimental Physiology's* animal use ethics checklist (Grundy, 2015), adhering to the standards for reporting animal experiments in the *The Journal of Physiology* and *Experimental Physiology*.

Experimental animals

Mice were housed in the University of Florida's Association for Assessment and Accreditation of Laboratory Animal Care (AAALAC)-accredited facility in the Biomedical Sciences Building. Wild type (WT) and DRA-KO (Slc26a3^{-/-}) mice bred on a C57BL/6 background were obtained from breeding pairs housed at the University of Florida. The DRA-KO mice (RRID:MGI:3697730) were initially generously provided by Dr. Manoocher Soleimani (University of Cincinnati). The generation of DRA-KO mice and offspring genotype has been described previously (Schweinfest et al., 2006). To offset the fluid and electrolyte losses associated with persistent diarrhea, and enhance survival past weaning, DRA-KO mice were maintained on a high calorie diet (Teklad diet 2919, Envigo, Cambridgeshire, UK) and Pedialyte was added to drinking water (50% vol/vol) (N. M. Walker et al., 2008; Xia et al., 2014). WT mice were given standard chow (Teklad diet 7919, Envigo) and sterile water until one week prior to experiments when they were switched to the same diet as DRA-KO mice. Male and female mice between 18 and 40 weeks of age with a mean body of mass of 26.3 ± 1.7 g, n = 16 (WT) and 27.8 ± 2.6 g, n = 14 (DRA-KO) were used. Mice were euthanized via inhalation of 100% CO_2 followed by cervical dislocation. The large intestine was dissected out and placed in ice cold buffer in preparation for transepithelial flux experiments.

Transepithelial fluxes

Unidirectional fluxes of Cl^- and I^- were simultaneously measured under symmetrical short-circuit current conditions across isolated pairs of tissue segments taken from the cecum and distal colon (4 cm of large intestine immediately proximal to the peritoneal border, representing the lower 30 % of the colon). Fat and connective tissue were carefully removed from the serosa and a pair of tissue segments prepared from each of the cecum and distal colon by opening longitudinally along the mesenteric border. Each of these segments were mounted as a flat sheet on a slider (P2304; Physiologic Instruments, San Diego, CA) and secured into a modified Ussing chamber (P2300; Physiologic Instruments, San Diego, CA),

exposing a gross surface area of 0.3 cm². Each tissue was bathed on either side in 4 ml of buffered saline maintained at 37°C and gassed with 95% O₂-5% CO₂ (pH 7.4). The buffered saline contained the following solutes (mM): Na⁺ 139.4, Cl⁻ 122.2, HCO₃⁻ 21.0, K⁺ 5.4, HPO₄²⁻ 2.4, Ca²⁺ 1.2, Mg²⁺ 1.2, H₂PO₄⁻ 0.6, SO₄²⁻ 0.5 and glucose 10. Additionally the buffer contained iodide (I⁻) at a concentration of 1.1 μM which was chosen to represent the physiological concentration of inorganic I⁻ previously determined in mouse serum (Kim et al., 2009). Automatic voltage clamps were used to continuously maintain the potential difference at 0 mV across each tissue segment (VCCM6 or VCC600; Physiologic Instruments, San Diego, CA).

Simultaneous Cl⁻ and I⁻ fluxes were measured by the addition of 0.09 μCi of ³⁶Cl (specific activity 571 μCi/mmol) and 0.27 μCi of ¹²⁵I (specific activity 138 mCi/mmol) to one side of the tissue, which was subsequently designated as the “hot side”. At 15 minute intervals for up to 105 minutes, 1 ml samples were taken from the opposing “cold side” for detection of tracers and recordings were made of short circuit current, I_{sc} (μA) and open circuit potential difference (mV). Buffer removed for sampling the “cold side” was immediately replaced with an equal volume of pre-warmed buffer. At the beginning and end of each experiment, a 50 μl sample was taken from the “hot side” to calculate the specific activity (dpm/mmol) of ³⁶Cl and ¹²⁵I. The activity of ³⁶Cl and ¹²⁵I was determined simultaneously in samples by liquid scintillation spectrophotometry (Beckman LS6500, Beckman-Coulter, Fullerton, CA). Buffer was added to samples where necessary to achieve a volume of 1 ml and mixed with 5 ml of scintillation cocktail (Ecoscint A, National Diagnostics, Atlanta, GA). ¹²⁵I produced a discrete energy spectra on the scintillation counter. The ¹²⁵I emissions detected by scintillation counting a series of external standards were confirmed to directly correlate (R² = 0.9993) with corresponding gamma emissions using a gamma counter (Wallac 1470 Wizard Gamma Counter, Perkin Elmer). The energy spectra produced by ¹²⁵I on the liquid scintillation counter was almost entirely separate from ³⁶Cl thus enabling both isotopes to be counted by liquid scintillation counting. Channel windows were set for counting each isotope with minimal overlap between the tracers’ energy spectra. A small spill of ³⁶Cl emission into the channel for ¹²⁵I measurement could not be avoided so was accounted for by subtracting estimated ³⁶Cl counts from the ¹²⁵I measurement window based on efficiency of ³⁶Cl in the ¹²⁵I measurement window and the measurement of ³⁶Cl from the ³⁶Cl measurement window which did not overlap with ¹²⁵I emissions. Energy spectra and counting efficiencies of isotopes in each window were obtained from single-labeled standards containing either 4951 cpm of ¹²⁵I (0.27 μCi) or 2465 cpm of ³⁶Cl (0.09 μCi). Additionally, the validity of dual label scintillation counting of ¹²⁵I and ³⁶Cl was confirmed by using two sets of external standards containing both isotopes, one in which the activity of ³⁶Cl was varied and one in which the activity of ¹²⁵I was varied. After a ratio of 5:1 (³⁶Cl: ¹²⁵I) measurements of ¹²⁵I were not as accurate. As such, far less ³⁶Cl was added to experimental chambers compared to ¹²⁵I, preventing ³⁶Cl activity exceeding that of ¹²⁵I in any sample and minimizing the spillover of ³⁶Cl into the ¹²⁵I measurement range.

To evaluate whether ¹²⁵I would successfully track changes to unidirectional ³⁶Cl fluxes, electrogenic Cl⁻ secretion was induced after 45 minutes (the end of the control period) by raising intracellular levels of cAMP through the addition of 10 μM forskolin (FSK) and 100 μM IBMX (3-isobutyl-1-methylxanthine) in DMSO to both mucosal and serosal baths. The

FSK/IBMX cocktail was prepared fresh each day and the final concentration of DMSO in each chamber was 0.05%.

Calculations and Statistics

Fluxes of Cl^- and I^- in either the secretory, serosal (S) to mucosal (M), (J_{sm}^{ion}) or the absorptive, mucosal to serosal, (J_{ms}^{ion}) directions were calculated from the changes to tracer activity in “cold side” samples after correcting for dilution by the replacement of buffer after sampling. Flux rates were expressed per cm^2 tissue per hour. Net fluxes (J_{net}^{ion}) were calculated as: $J_{net}^{ion} = J_{ms}^{ion} - J_{sm}^{ion}$ from tissues paired based on average transepithelial conductance (G_T ; mS/cm^2) during the initial control period (Period I; i.e. time points preceding FSK/IBMX treatment (0–45 min)) where G_T between tissue pairs did not exceed $\pm 25\%$. Net fluxes with a negative sign indicated overall secretion whereas positive values represented net absorption. G_T was calculated from I_{sc} and transepithelial potential difference using Ohm’s law. Data are presented as the mean (SD). Differences between average J_{net}^{ion} , J_{ms}^{ion} and J_{sm}^{ion} by WT and DRA KO epithelia in the control period were assessed by unpaired t-test or Mann-Whitney Rank sum test where the assumption of normality was violated (as determined by Shapiro-Wilk’s test) or Welch’s t-test where variances were unequal (as determined by the Brown-Forsythe test). To evaluate the effect of FSK/IBMX application on net Cl^- and I^- transport, the average J_{net}^{ion} during the experimental period (i.e. following the addition of FSK/IBMX (Period II, 60–105 min)), and Period I (the control period) were compared by paired T-test. To evaluate the unidirectional flux responses to FSK/IBMX, each individual 15 min sampling point in Period II (60–105 min) was compared to the average of sample time points in Period I (0–45 min) by repeated measures one-way ANOVA and, where appropriate, Holm-Sidak post-hoc tests were used to identify differences between individual time points in Period II and the control period. In cases where the assumptions of normality (as determined by Shapiro-Wilk’s test) and/or equality of variance (as determined by the Brown-Forsythe test) were violated, the Friedman repeated measures ANOVA was performed on ranks and Dunn’s post-hoc test used to identify differences between specific time points and the control period. Regression analysis was performed on average J^{Cl} and J^I values in each tissue for each time period (Period I and Period II) to evaluate the relationship between the unidirectional fluxes of Cl^- (J^{Cl}) and I^- (J^I). Multiple regression analysis was used to compare the slopes and intercepts of the relationships between J^{Cl} and J^I from WT and DRA-KO mice, and cecum and distal colon. In all tests statistical significance was accepted at $P < 0.05$. Multiple regression analysis was performed using Minitab 18. ANOVAs were performed and figures drawn with Sigmaplot 13.

Results

Chloride and iodide fluxes in WT and DRA-KO mice

During the control period (0–45 min), the cecum and distal colon from WT mice exhibited negligible net Cl^- transport across paired tissues; -0.10 (2.87) and 1.58 (4.38) $\mu\text{mol}/\text{cm}^2/\text{h}$,

respectively (n = 6). Net fluxes were calculated from unidirectional flux data presented in Figure 1 and Figure 2 (Panels A – D). A small net secretion of I⁻ was determined across the WT cecum and distal colon; -6.83 (10.29) and -15.60 (22.71) pmol/cm²/h, respectively (n = 6). There was a distinct net secretion of Cl⁻ in both the cecum and distal colon of DRA KO mice which was significantly different from net Cl⁻ transport in WT mice (p > 0.001). Net Cl⁻ transport in the absence of DRA was -6.99 (1.03) (n = 7) and -4.62 (0.69) μmol/cm²/h (n = 6) in the cecum and distal colon, respectively. These values were comparable to the substantial I_{sc} of -5.93 (1.20) (n = 14) and -3.80 (0.6) (n=14) μeq/cm²/h in each respective segment. Net I⁻ transport by the DRA-KO large intestine was -18.53 (11.61) (n = 7) in the cecum and -14.94 (9.09) (n = 6) pmol/cm²/h in the distal colon which was, however, not significantly different from the net I⁻ transport in WT mice (p = 0.084 and p = 0.950 respectively).

The absorptive (J_{ms}) fluxes of Cl⁻ and I⁻ were lower in both the cecum and distal colon of DRA-KO mice compared to WT cecum and distal colon; the absence of DRA resulted in a significant 79 % decrease in J_{ms}^{Cl} and a 50 % decrease in J_{ms}^I in the ceca (Figure 1, A and B) (p < 0.001), with a significant decrease of 65 % of J_{ms}^{Cl} and 34 % of J_{ms}^I in the distal colon (Figure 2, A and B) (p < 0.001 and p = 0.010 respectively). Additionally, the secretory (J_{sm}) flux in the control period for both Cl⁻ and I⁻ was lower in the absence of DRA in both the cecum and the distal colon, however this effect was greatest in the cecum where the absence of DRA resulted in a 45% and a 41% decrease in J_{sm}^{Cl} and J_{sm}^I , respectively (Figure 1, C and D). In the distal colon J_{sm}^{Cl} and J_{sm}^I were only decreased 15% and 17% (Figure 2, C and D). Both the DRA-KO cecum and distal colon exhibited a lower I_{sc} in the control period than WT cecum, however, whereas DRA-KO ceca had a reduced G_T relative to the WT (Figure 1, E and F), G_T was higher in the DRA-KO distal colon than WT distal colon (Figure 2 E and F).

The effect of FSK/IBMX on chloride and iodide fluxes in WT and DRA-KO mice

In the WT cecum, application of FSK/IBMX induced significant net Cl⁻ and I⁻ secretion of -7.39 (4.63) μmol/cm²/h and -30.66 (24.54) pmol/cm²/h (n = 6), respectively, compared to the control period (p = 0.014 and p = 0.021 for Cl⁻ and I⁻ respectively). This was due to reductions in both the absorptive (J_{ms}^{ion}) and secretory (J_{sm}^{ion}) fluxes of Cl⁻ and I⁻ (Figure 1, A and C), where J_{ms}^{Cl} and J_{ms}^I were decreased 70% and 60%, respectively, alongside a 30% reduction to both J_{sm}^{Cl} and J_{sm}^I . By comparison, the stimulation of cAMP by FSK/IBMX had less of an effect on the DRA-KO cecum resulting in no significant change to net Cl⁻ secretion but a significant net secretion of I⁻ (31.27 (7.30) pmol/cm²/h; n = 7) relative to the control period (p = 0.018). In terms of unidirectional fluxes, a small, but significant, increase was observed in J_{ms}^{Cl} and J_{sm}^I (p < 0.001 for both) (Figure 1, B and D). Correspondingly, I_{sc} and G_T responded differently to FSK/IBMX in DRA-KO cecum compared to WT cecum. Significant decreases in I_{sc} were detected immediately following the application of FSK and IBMX in WT cecum only (p < 0.001), whereas a significant increase was detected in DRA-KO cecum (p < 0.001) after a slight initial drop (Figure 1, E). A significant reduction in G_T

was detected in WT cecum after 45 minutes of FSK/IBMX exposure ($p < 0.001$), whereas G_T in the DRA-KO cecum continued to increase following a trend seen throughout the preceding control period (Figure 1, F).

In WT distal colon (Figure 2), FSK/IBMX induced an overall net Cl^- secretion of -5.50 (5.58) $\mu\text{mol}/\text{cm}^2/\text{h}$ ($n = 6$) which was significantly higher compared to the control period ($p = 0.032$). Net I^- secretion also increased to -31.38 (23.42) $\text{pmol}/\text{cm}^2/\text{h}$ ($n = 6$), but this was not significant relative to the control period ($p = 0.392$). There was a significant decrease in average J_{ms}^{Cl} and J_{ms}^I by 57% and 42%, respectively ($p = 0.002$ and $p = 0.012$ respectively) (Figure 2, A), however, no effect was observed on either of the average secretory fluxes ($p = 0.935$ for J_{sm}^{Cl} and $p = 0.598$ for J_{sm}^I) (Figure 2, C). The application of FSK/IBMX to DRA-KO distal colon induced a respective net secretion of Cl^- and I^- of -9.75 (3.11) $\mu\text{mol}/\text{cm}^2/\text{h}$ and -44.99 (25.06) $\text{pmol}/\text{cm}^2/\text{h}$ ($n = 6$), which was significant relative to the control period ($p = 0.007$ and $p = 0.008$, respectively). Predominantly, no effect on J_{ms}^{Cl} and J_{ms}^I was observed; there was no significant difference between the control period average J_{ms}^{Cl} and J_{ms}^I and the period II J_{ms}^{Cl} and J_{ms}^I when compared by a paired T-test ($p = 0.656$ and $p = 0.066$), however repeated measures ANOVA between measured J_{ms}^{Cl} and J_{ms}^I at 15 minute time points after the addition of FSK/IBMX compared to the average of the control period were significant when tested by ANOVA ($p = 0.001$ and $p = 0.019$ for J_{ms}^{Cl} and J_{ms}^I respectively with a significant difference to the control only detected at 60 minutes for J_{ms}^{Cl} , $p = 0.012$ with Holm-Sidak method post-hoc test (Figure 2, B). In contrast, J_{sm}^{Cl} and J_{sm}^I were significantly increased by an average of 52% and 34%, respectively (Figure 2, D) when compared to the control by a repeated measures T-test ($p = 0.006$ and $p = 0.003$ respectively). The responses of I_{sc} and G_T in DRA-KO distal colon were similar to the response of WT distal colon; a dramatic, significant, drop in I_{sc} was observed in time points following the application of FSK/IBMX ($p < 0.001$) (Figure 2, E) and G_T rose slightly ($p = 0.015$), which was significant at 30 minutes after FSK/IBMX application ($p = 0.003$) (Figure 2, F).

Relationships between transmural ^{36}Cl and ^{125}I transport

A strong, significant correlation was observed between both unidirectional fluxes of chloride and iodide across the cecum of WT and DRA-KO mice ($p < 0.001$), with an R^2 of 0.93 and 0.90, respectively (Figure 3). The correlations between J^{Cl} and J^I fluxes in the distal colon of WT and DRA-KO mice were slightly weaker, but still highly significant ($p < 0.001$), each with a respective R^2 of 0.72 and 0.87 (Figure 4). When points from both cecum and distal colon of WT and DRA-KO mice were combined together (data not shown), this strong correlation between J^{Cl} and J^I fluxes was maintained and the relationship, as defined by linear regression, was: $J^I = 4.195 \cdot J^{Cl} + 24.41$, with an R^2 of 0.86 ($P < 0.001$). Each of the intercepts shown in Figures 3 and 4 was significantly different from zero. When the slope and intercepts of regressions were compared they were found to be significantly different between WT (Figure 3, A) and DRA KO cecum (Figure 3, B), but not between genotypes

for the distal colon (Figure 4). The slope and intercept of regressions were significantly different between the cecum (Figure 3, A) and distal colon (Figure 4, A) for WT, but not DRA-KO mice.

Discussion

The escalating cost of ^{36}Cl has made its use as a tracer of epithelial Cl^- transport prohibitive. This study therefore examined whether ^{125}I was able to serve as a reliable surrogate for ^{36}Cl and the measurement of transepithelial Cl^- fluxes across the mouse cecum and distal colon. We found the fluxes of ^{125}I consistently correlated very well with ^{36}Cl in both cecum and distal colon in the presence and absence of the main apical $\text{Cl}^-/\text{HCO}_3^-$ exchanger, DRA. We also showed, for the first time, that DRA makes a significant contribution to I^- transport by the mouse large intestine. The correlation between ^{36}Cl and ^{125}I fluxes was maintained following stimulation of electrogenic anion secretion by cAMP revealing that net Cl^- secretion was achieved through a reduction in unidirectional Cl^- (and I^-) absorption rather than an increase in secretion, which is critically important considering the transporters and channels responsible for Cl^- secretion are targets for antidiarrheal drugs (Thiagarajah, Donowitz, & Verkman, 2015). Notably, the details of these responses from the unidirectional Cl^- (and I^-) fluxes would not have been discernable from measuring net Cl^- transport or I_{sc} alone. As such, this study highlights the value of measuring unidirectional ion fluxes and demonstrates that ^{125}I can function as an acceptable alternative tracer to ^{36}Cl for examining transepithelial Cl^- secretion across segments of the mouse large intestine.

To be an acceptable surrogate for tracing Cl^- fluxes across a heterogeneous native epithelium, ^{125}I should be able to substitute for Cl^- on all transporters which accept Cl^- as a substrate. The primary transporter responsible for Cl^- absorption in the cecum is DRA; where it has previously been shown that $\text{Cl}^-/\text{HCO}_3^-$ exchange and net Cl^- absorption by the cecum are abolished in DRA-KO mice (Alper et al., 2011; Freel et al., 2013; Whittamore et al., 2013). In this study, the absence of DRA similarly reduced J_{ms}^{Cl} . This decrease in Cl^- absorption was mirrored by a similar reduction in J_{ms}^{I} suggesting DRA might also be contributing to a significant proportion of I^- absorption. To our knowledge, it has never been tested whether DRA is capable of transporting iodide in heterologous expression systems. However, thyroxine, a hormone that is reduced in iodine deficiency (Fukuda, Yasuda, Greer, Kutas, & Greer, 1975), has been shown to down-regulate DRA mRNA expression in Caco-2 cells (Alrefai et al., 2001), possibly indicating a broader physiological role for DRA in the intestine. ^{125}I fluxes in DRA-KO tissues demonstrated that I^- was likely also transported through other chloride transport pathways. For example, changes in J^{Cl} induced by FSK/IBMX correlated well with J^{I} even in DRA-KO mice, consistent with I^- being a substrate for other prominent cAMP-regulated Cl^- transporters in the large intestine, such as the Cystic Fibrosis Transmembrane Conductance Regulator, CFTR (Dawson, Smith, & Mansoura, 1999; McCarty, 2000). Very little is known about I^- handling by the large intestine but in the rat small intestine I^- absorption has been attributed to the apical sodium-iodide symporter, NIS (Slc5a5) (Nicola et al., 2009) which operates independently of Cl^- (Eskandari et al., 1997). The expression of NIS mRNA does extend into the large intestine of the deer mouse (*Peromyscus maniculatus*) (Cheng et al., 2007), but whether this is also the case for the

laboratory mouse has not been documented. Independent of the presence of DRA, any functional contribution of apical NIS to I^- absorption by the large intestine would appear to be minimal based on the consistent correlations observed between J^{Cl} and J^I in DRA-KO tissues and following stimulation of cAMP.

From the present findings we suggest that ^{125}I can serve as a useful surrogate for measuring transepithelial Cl^- fluxes but with a few notes of caution. Firstly, the intercept of the relationship between J^I and J^{Cl} was significantly different from zero in both cecum and distal colon of WT and DRA KO mice. This extrapolation suggests that in the complete absence of Cl^- transport some I^- transport continues suggesting a small, but significant fraction of I^- fluxes are Cl^- independent. Thus, any changes to I^- transport should be interpreted with care as they may not necessarily be representative of alterations in Cl^- transport. Secondly, there were also significant differences in the slope and intercepts between J^I and J^{Cl} in both tissues and genotypes. As such, the behavior of J^I in relation to J^{Cl} in one segment of the intestine cannot necessarily be assumed as the same in another, thus requiring investigators to independently validate the use of I^- as a substitute for Cl^- for the segment(s) being studied. Additionally, the slope and intercepts of J^I and J^{Cl} were significantly different between WT and DRA-KO mice, but only in the cecum. This suggests that it may not be valid to directly compare J^I between a WT mouse and its transgenic counterpart and conclude that it fully represents J^{Cl} in the latter. Although the differences observed between slopes and intercepts of different tissue types and genotypes were statistically significant, the magnitude of these differences were not large. A regression on a combination of all fluxes measured in both cecum and distal colon from WT and DRA-KO mice suggested that changes to J^I can explain 86% of the variability in J^{Cl} across this study. Finally, another important factor to consider is the potential presence of transporters with an affinity for either Cl^- or I^- , but not both. For example, the $Na^+-K^+-2Cl^-$ co-transporter NKCC1 (Slc12a2) is one of the major Cl^- transport pathways supporting cAMP-stimulated Cl^- secretion for which I^- is considered a poor substrate (O'Grady, Palfrey, & Field, 1987). If I^- is not generally conducted through NKCC1 then significant changes in J^{Cl} through this co-transporter may not necessarily be revealed by J^I . In the present study, however, this may have been of little consequence since cAMP stimulated net Cl^- secretion was achieved almost entirely through a reduction in J_{ms}^{Cl} , rather than an increase to J_{sm}^{Cl} , as seen previously in the rabbit, guinea pig and lizard colon (Díaz & Lorenzo, 1991; M Hatch et al., 1994; Marguerite Hatch et al., 1993; Yajima et al., 1988). This might explain why the relationships between I^- and Cl^- fluxes remained so remarkably consistent in both the control period and following treatment with FSK/IBMX. Whether this agreement between epithelial Cl^- and I^- fluxes occurs across species remains to be seen. The situation may also be more complicated in the small intestine, and the distal ileum where J_{sm}^{Cl} increases (and J_{ms}^{Cl} simultaneously decreases) in response to FSK/IBMX (Whittamore & Hatch, 2017). Similarly, the sodium-iodide symporter, NIS which is predominantly expressed in the small intestine (Donowitz et al., 2007; Nicola et al., 2009), and transports I^- independently of Cl^- (Eskandari et al., 1997), may also be a complicating factor when attempting to utilize J^I in place of J^{Cl} in the small intestine.

The use of ^{125}I can be invaluable for interpreting transepithelial I_{sc} and net Cl^- transport since the former is an amalgamation of the major net electrogenic ion fluxes including Cl^- . In this study, a dramatic drop in I_{sc} was observed in response to FSK/IBMX in the distal colon of both WT and DRA-KO mouse (Figure 2, E) and this corresponded with increasing net Cl^- (and I^-) secretion. Activation of apical CFTR by cAMP in conjunction with NKCC1 allows chloride to exit the cell which should register as an increase in $J_{\text{sm}}^{\text{Cl}}$. However, both ^{125}I and ^{36}Cl , revealed the change in net Cl^- transport appeared to take place through two distinct mechanisms depending on the presence or absence of DRA. In WT distal colon and cecum there was a reduction in the absorptive fluxes of Cl^- and I^- , resulting in overall net secretion in response to cAMP (Figure 2, A and C), with no corresponding stimulation of $J_{\text{sm}}^{\text{Cl}}$ or J_{sm}^{I} . In DRA-KO distal colon, however, $J_{\text{sm}}^{\text{Cl}}$ (and J_{sm}^{I}) increased with no change in $J_{\text{ms}}^{\text{Cl}}$ or J_{ms}^{I} (Figure 2, B and D). These findings indicate that in the presence of functional DRA the increase in net Cl^- secretion in the mouse large intestine takes place exclusively through the reduction of (DRA-mediated) Cl^- absorption, rather than a stimulation of $J_{\text{sm}}^{\text{Cl}}$ involving apical CFTR in series with NKCC1. This reduction in $J_{\text{ms}}^{\text{Cl}}$ by the large intestine may occur through the endocytosis of DRA, as demonstrated for the mouse jejunum and Caco-2 cells after the stimulation of cAMP (Musch, Arvans, Wu, & Chang, 2009). Indeed, this is supported here in the large intestine by the observation that cAMP reduced $J_{\text{ms}}^{\text{Cl}}$ in the WT cecum and distal colon down to rates similar to those observed in DRA-KOs while the response of $J_{\text{ms}}^{\text{Cl}}$ to cAMP stimulation was muted in DRA KO epithelia (Figure 1 and Figure 2), as similarly observed in the distal ileum (Whittamore and Hatch, 2017).

Relatively few studies have directly measured unidirectional Cl^- fluxes by the mouse intestine in response to FSK, of which even fewer have examined the large intestine. In the jejunum, however, previous studies observed increases in secretory Cl^- fluxes as well as increases or decreases in absorptive fluxes producing an overall stimulation of net Cl^- secretion in response to elevated levels of intracellular cAMP (Gawenis et al., 2002; Seidler et al., 2008). Since cAMP affects both absorptive and secretory processes this highlights the utility of measuring unidirectional fluxes with a tracer in order to reveal such details, which would have otherwise been missed by relying on an index of net transport such as I_{sc} . This is particularly significant concerning the development of anti-diarrheal therapeutic agents which target inhibition of the secretory process, such as CFTR (Thiagarajah et al., 2015).

In conclusion, this study reveals that ^{125}I is an acceptable tracer for transepithelial Cl^- transport thus offering an alternative tool for continuing research into the Cl^- transport mechanism of the mouse large intestine. We demonstrated that I^- appears to share a number of common Cl^- transport pathways in the mouse large intestine, including, for the first time, the $\text{Cl}^-/\text{HCO}_3^-$ exchanger DRA, which contributes significantly to I^- fluxes across the cecum and distal colon. Both J^{I} and J^{Cl} correlated well in the presence and absence of DRA, and following the induction of cAMP-stimulated secretion thus further demonstrating the utility of $^{125}\text{I}^-$. We also showed that cAMP-stimulated net Cl^- secretion by the WT mouse large intestine was achieved entirely through a reduction in Cl^- absorption rather than an increase in secretion, thus highlighting the value of measuring both unidirectional Cl^-

fluxes. The use of $^{125}\text{I}^-$ as a surrogate tracer for transepithelial chloride transport will be valuable for future research on transepithelial Cl^- transport by providing a much cheaper, realistic alternative to the prohibitive cost of $^{36}\text{Cl}^-$. For example, in the present study we used \$536 worth of $^{36}\text{Cl}^-$, relative to just \$4 of $^{125}\text{I}^-$!

Acknowledgements

We thank Maureen Mohan for technical assistance and animal husbandry.

Funding

This study was supported by grants DK088892 and DK108755 to M. Hatch from the National Institutes of Health.

References

- Alper SL, Stewart AK, Vandorpe DH, Clark JS, Zachary Horack R, Simpson JE, ... Clarke LL (2011). Native and recombinant Slc26a3 (downregulated in adenoma, Dra) do not exhibit properties of 2Cl⁻/1HCO₃⁻ exchange. *AJP: Cell Physiology*, 300(2), C276–C286. 10.1152/ajpcell.00366.2010 [PubMed: 21068358]
- Alrefai WA, Tyagi S, Mansour F, Saksena S, Syed I, Ramaswamy K, & Dudeja PK (2001). Sulfate and chloride transport in Caco-2 cells: differential regulation by thyroxine and the possible role of DRA gene. *American Journal of Physiology: Gastrointestinal and Liver Physiology*, 280(4), G603–G613. 10.1152/ajpgi.2001.280.4.G603 [PubMed: 11254486]
- Bridges RJ, Rummel W, & Simon B (1983). Forskolin induced chloride secretion across the isolated mucosa of rat colon descendens. *Naunyn-Schmiedeberg's Archives of Pharmacology*, 323(4), 355–360. 10.1007/BF00572436
- Cheng Q, Smith EE, Liu F, Gentle A, Hooper MJ, & Anderson TA (2007). Effects of perchlorate on sodium-iodide symporter and pendrin gene expression in deer mice. *Environmental Toxicology*, 22(4), 390–398. 10.1002/tox.20271 [PubMed: 17607730]
- Cheval L, & Doucet A (1990). Measurement of Na-K-ATPase-mediated rubidium influx in single segments of rat nephron. *American Journal of Physiology: Renal Physiology*, 259(1), F111–F121. 10.1152/ajprenal.1990.259.1.F111
- Clarke LL (2009). A guide to Ussing chamber studies of mouse intestine. *American Journal of Physiology: Gastrointestinal and Liver Physiology*, 296(6), G1151–G1166. 10.1152/ajpgi.90649.2008 [PubMed: 19342508]
- Curran PF (1960). Na, Cl, and water transport by rat ileum in vitro. *Journal of General Physiology*, 43(6), 1137–1960. 10.1085/jgp.43.6.1137 [PubMed: 13813357]
- Dawson D, Smith S, & Mansoura M (1999). CFTR: Mechanism of anion conduction. *Physiological Reviews*, 79(1), S47–S75. 10.1152/physrev.1999.79.1.S47 [PubMed: 9922376]
- Díaz M, & Lorenzo A (1991). Coexistence of absorptive and secretory NaCl processes in the isolated lizard colon: effects of cyclic AMP. *Zoological Science*, 8, 477–484.
- Donowitz M, Singh S, Salahuddin FF, Hogema BM, Chen Y, Gucek M, ... Li X (2007). Proteome of murine jejunal brush border membrane vesicles. *Journal of Proteome Research*, 6(10), 4068–4079. 10.1021/pr0701761 [PubMed: 17845021]
- Eskandari S, Loo DDF, Dai G, Levy O, Wright EM, & Carrasco N (1997). Thyroid Na⁺ / I⁻ symporter. Mechanism, stoichiometry, and specificity. *The Journal of Biological Chemistry*, 272(43), 27230–27238. 10.1074/jbc.272.43.27230 [PubMed: 9341168]
- Field M (1971). Ion transport in rabbit ileal mucosa. II. Effects of cyclic 3',5'-AMP. *American Journal of Physiology*, 221(4), 992–997. 10.1152/ajplegacy.1971.221.4.992 [PubMed: 4329427]
- Flagella M, Clarke LL, Marian L, Erway LC, Ralph A, Andringa A, ... Shull GE (1999). Mice lacking the basolateral Na-K-2Cl cotransporter have impaired epithelial chloride secretion and are profoundly deaf. *The Journal of Biological Chemistry*, 274(38), 26946–26955. 10.1074/jbc.274.38.26946 [PubMed: 10480906]

- Freel RW, Whittamore JM, & Hatch M (2013). Transcellular oxalate and Cl^- absorption in mouse intestine is mediated by the DRA anion exchanger Slc26a3, and DRA deletion decreases urinary oxalate. *American Journal of Physiology: Gastrointestinal and Liver Physiology*, 305(7), G520–G527. 10.1152/ajpgi.00167.2013 [PubMed: 23886857]
- Fukuda H, Yasuda N, Greer MA, Kutas M, & Greer SE (1975). Changes in plasma thyroxine, triiodothyronine, and TSH during adaptation to iodine deficiency in the rat. *Endocrinology*, 97(2), 307–314. 10.1210/endo-97-2-307 [PubMed: 1157754]
- Gawenis LR, Ledoussal C, Judd LM, Prasad V, Alper SL, Stuart-Tilley A, ... Shull GE (2004). Mice with a targeted disruption of the AE2 $\text{Cl}^-/\text{HCO}_3^-$ exchanger are achlorhydric. *The Journal of Biological Chemistry*, 279(29), 30531–9. 10.1074/jbc.M403779200 [PubMed: 15123620]
- Gawenis LR, Stien X, Shull GE, Schultheis PJ, Woo AL, Walker NM, & Clarke LL (2002). Intestinal NaCl transport in NHE2 and NHE3 knockout mice. *American Journal of Physiology: Gastrointestinal and Liver Physiology*, 282(5), G776–G784. 10.1152/ajpgi.00297.2001 [PubMed: 11960774]
- Grundy D (2015). Principles and standards for reporting animal experiments in *The Journal of Physiology and Experimental Physiology*. *Journal of Physiology*, 593(12), 2547–2549. 10.1113/JP270818 [PubMed: 26095019]
- Gujral T, Kumar A, Priyamvada S, Saksena S, Gill RK, Hodges K, ... Dudeja PK (2015). Mechanisms of DRA recycling in intestinal epithelial cells: effect of enteropathogenic *E. coli*. *American Journal of Physiology: Cell Physiology*, 309(12), C835–C846. 10.1152/ajpcell.00107.2015 [PubMed: 26447204]
- Hatch M, Freel RW, & Vaziri ND (1993). Characteristics of the transport of oxalate and other ions across rabbit proximal colon. *Pflügers Archiv European Journal of Physiology*, 423(3–4), 206–212. 10.1007/BF00374396 [PubMed: 8391680]
- Hatch M, Freel RW, & Vaziri ND (1994). Mechanisms of oxalate absorption and secretion across the rabbit distal colon. *Pflügers Archiv European Journal of Physiology*, 426(1–2), 101–109. 10.1007/BF00374677 [PubMed: 8146012]
- Hatch M, Freel RW, & Vaziri ND (1998). Local upregulation of colonic angiotensin II receptors enhances potassium excretion in chronic renal failure. *American Journal of Physiology: Renal Physiology*, 274(2 Pt 2), F275–82. 10.1152/ajprenal.1998.274.2.F275
- Kim YH, Pham TD, Zheng W, Hong S, Baylis C, Pech V, ... Wall SM (2009). Role of pendrin in iodide balance: going with the flow. *American Journal of Physiology: Renal Physiology*, 297(4), F1069–F1079. 10.1152/ajprenal.90581.2008 [PubMed: 19605545]
- Kravtsov DV, Ahsan MK, Kumari V, van Ijzendoorn SCD, Reyes-Mugica M, Kumar A, ... Ameen NA (2016). Identification of intestinal ion transport defects in microvillus inclusion disease. *American Journal of Physiology: Gastrointestinal and Liver Physiology*, 311(1), G142–G155. 10.1152/ajpgi.00041.2016 [PubMed: 27229121]
- Kumar A, Hecht C, Priyamvada S, Anbazhagan AN, Alakkam A, Borthakur A, ... Dudeja PK (2014). Probiotic *Bifidobacterium* species stimulate human SLC26A3 gene function and expression in intestinal epithelial cells. *American Journal of Physiology: Cell Physiology*, 307(12), C1084–C1092. 10.1152/ajpcell.00194.2014 [PubMed: 25143346]
- Li H, Sheppard DN, & Hug MJ (2004). Transepithelial electrical measurements with the Ussing chamber. *Journal of Cystic Fibrosis*, 3(SUPPL. 2), 123–126. 10.1016/j.jcf.2004.05.026 [PubMed: 15463943]
- McCarty NA (2000). Permeation through the CFTR chloride channel. *The Journal of Experimental Biology*, 203, 1947–1962. [PubMed: 10851114]
- Moran O, & Zegarra-Moran O (2008). On the measurement of the functional properties of the CFTR. *Journal of Cystic Fibrosis*, 7(6), 483–494. 10.1016/j.jcf.2008.05.003 [PubMed: 18818127]
- Musch MW, Arvans DL, Wu GD, & Chang EB (2009). Functional coupling of the downregulated in adenoma Cl^- /base exchanger DRA and the apical Na^+/H^+ exchangers NHE2 and NHE3. *American Journal of Physiology: Gastrointestinal and Liver Physiology*, 296(2), G202–10. 10.1152/ajpgi.90350.2008 [PubMed: 19056765]

- Nicola JP, Basquin C, Portulano C, Reyna-Neyra A, Paroder M, & Carrasco N (2009). The Na⁺/I⁻ symporter mediates active iodide uptake in the intestine. *American Journal of Physiology: Cell Physiology*, 296(4), C654–C662. 10.1152/ajpcell.00509.2008 [PubMed: 19052257]
- Nobles M, Diener M, & Rummel W (1991). Segment-specific effects of the heat-stable enterotoxin of *E. coli* on electrolyte transport in the rat colon. *European Journal of Pharmacology*, 202, 201–211. 10.1016/0014-2999(91)90295-2 [PubMed: 1724966]
- O'Grady SM, Palfrey HC, & Field M (1987). Characteristics and functions in epithelial tissues of Na-K-Cl cotransport. *The American Journal of Physiology: Cell Physiology*, 253(2), C177–C192. 10.1152/ajpcell.1987.253.2.C177
- Oppermann M, Mizel D, Kim SM, Chen L, Faulhaber-Walter R, Huang Y, ... Castrop H (2007). Renal function in mice with targeted disruption of the A isoform of the Na-K-2Cl co-transporter. *Journal of the American Society of Nephrology*, 18(2), 440–448. 10.1681/ASN.2006091070 [PubMed: 17215439]
- Ribeiro R, Heinke B, & Diener M (2001). Cell volume-induced changes in K⁺ transport across the rat colon. *Acta Physiologica Scandinavica*, 171(4), 445–458. 10.1046/j.1365-201X.2001.00806.x [PubMed: 11421860]
- Saksena S, Tyagi S, Goyal S, Gill RK, Alrefai WA, Ramaswamy K, & Dudeja PK (2010). Stimulation of apical Cl⁻/HCO₃⁻(OH⁻) exchanger, SLC26A3 by neuropeptide Y is lipid raft dependent. *American Journal of Physiology: Gastrointestinal and Liver Physiology*, 299(6), G1334–G1343. [PubMed: 20884887]
- Schweinfest CW, Spyropoulos DD, Henderson KW, Kim JH, Chapman JM, Barone S, ... Soleimani M (2006). Slc26a3 (dra)-deficient mice display chloride-losing diarrhea, enhanced colonic proliferation, and distinct up-regulation of ion transporters in the colon. *Journal of Biological Chemistry*, 281(49), 37962–37971. 10.1074/jbc.M607527200 [PubMed: 17001077]
- Seidler U, Rottinghaus I, Hillesheim J, Chen M, Riederer B, Krabbenhoft A, ... Soleimani M (2008). Sodium and chloride absorptive defects in the small intestine in Slc26a6 null mice. *Pflügers Archiv European Journal of Physiology*, 455(4), 757–766. 10.1007/s00424-007-0318-z [PubMed: 17763866]
- Talbot C, & Lytle C (2010). Segregation of Na/H exchanger-3 and Cl/HCO₃ exchanger SLC26A3 (DRA) in rodent cecum and colon. *American Journal of Physiology: Gastrointestinal and Liver Physiology*, 299(2), G358–G367. 10.1152/ajpgi.00151.2010 [PubMed: 20466943]
- Thiagarajah JR, Donowitz M, & Verkman AS (2015). Secretory diarrhoea: Mechanisms and emerging therapies. *Nature Reviews Gastroenterology and Hepatology*, 12(8), 446–457. 10.1038/nrgastro.2015.111 [PubMed: 26122478]
- Venglarik CJ, Bridges RJ, & Frizzell RA (1990). A simple assay for agonist-regulated Cl and K conductances in salt-secreting epithelial cells. *The American Journal of Physiology*, 259(6), 605–615. 10.1152/ajpcell.1990.259.2.C358
- Walker J, Jijon HB, Churchill T, Kulka M, & Madsen KL (2003). Activation of AMP-activated protein kinase reduces cAMP-mediated epithelial chloride secretion. *American Journal of Physiology: Gastrointestinal and Liver Physiology*, (780), 1–39. 10.1152/ajpgi.00077.2003
- Walker NM, Simpson JE, Yen P-F, Gill RK, Rigsby EV, Brazill JM, ... Clarke LL (2008). Down-regulated in adenoma Cl⁻/HCO₃⁻ exchanger couples with Na⁺/H⁺ exchanger 3 for NaCl absorption in murine small intestine. *Gastroenterology*, 135(5), 1645–1653. 10.1053/j.gastro.2008.07.083 [PubMed: 18930060]
- Wang ZH, Wang T, Petrovic S, Tuo BG, Riederer B, Barone S, ... Soleimani M (2005). Renal and intestinal transport defects in Slc26a6-null mice. *American Journal of Physiology: Cell Physiology*, 288(4), C957–C965. 10.1152/ajpcell.00505.2004. [PubMed: 15574486]
- Whittamore JM, Freel RW, & Hatch M (2013). Sulfate secretion and chloride absorption are mediated by the anion exchanger DRA (Slc26a3) in the mouse cecum. *American Journal of Physiology: Gastrointestinal and Liver Physiology*, 305(2), G172–G184. 10.1152/ajpgi.00084.2013 [PubMed: 23660504]
- Whittamore JM, & Hatch M (2017). Loss of the anion exchanger DRA (Slc26a3), or PAT1 (Slc26a6), alters sulfate transport by the distal ileum and overall sulfate homeostasis. *American Journal of Physiology: Gastrointestinal and Liver Physiology*, 313(3), G166–G179. 10.1152/ajpgi.00079.2017 [PubMed: 28526688]

- Xia WL, Yu Q, Riederer B, Singh AK, Engelhardt R, Yeruva S, ... Seidler U (2014). The distinct roles of anion transporters Slc26a3 (DRA) and Slc26a6 (PAT-1) in fluid and electrolyte absorption in the murine small intestine. *Pflügers Archiv-European Journal of Physiology*, 466(8), 1541–1556. 10.1007/s00424-013-1381-2 [PubMed: 24233434]
- Yajima T, Suzuki T, & Suzuki Y (1988). Synergism between calcium-mediated and cyclic AMP-mediated activation of chloride secretion in isolated guinea pig distal colon. *The Japanese Journal of Physiology*, 38(4), 427–443. 10.2170/jjphysiol.38.427 [PubMed: 2907061]

New findings

What is the central question of this study?

The tracer $^{36}\text{Cl}^-$ (chloride), currently used to measure transepithelial Cl^- fluxes, has become prohibitively expensive threatening its future use. $^{125}\text{I}^-$ (iodide), previously validated alongside $^{36}\text{Cl}^-$ as a tracer of Cl^- efflux by cells, has not been tested as a surrogate for $^{36}\text{Cl}^-$ across epithelia.

What is the main finding and its importance?

We demonstrate that $^{125}\text{I}^-$ can serve as an inexpensive replacement for measuring Cl^- transport across mouse large intestine, tracking Cl^- transport in response to cAMP stimulation (inducing Cl^- secretion) in the presence and absence of the main gastrointestinal $\text{Cl}^-/\text{HCO}_3^-$ exchanger, DRA.

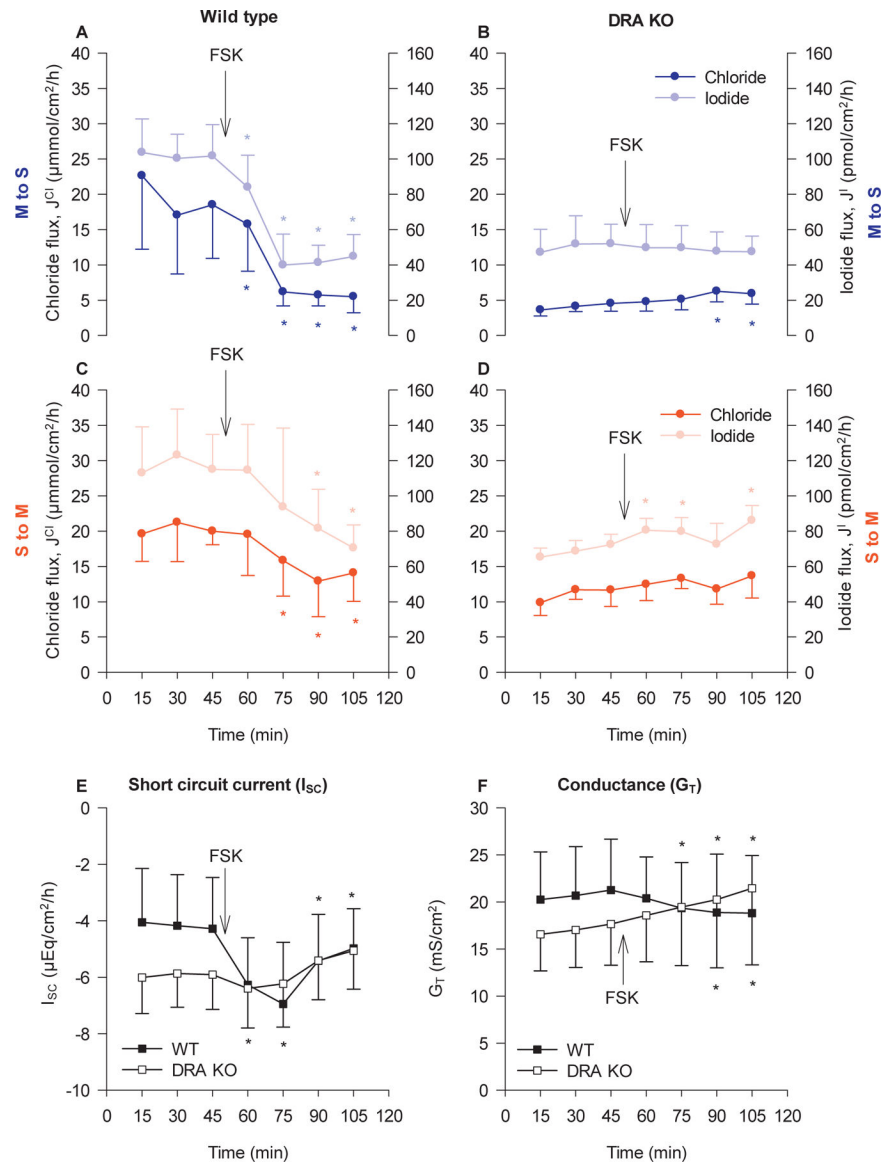


Figure 1. Chloride and iodide fluxes across the WT and DRA-KO mouse cecum.

Unidirectional J^{Cl} and J^I measured in the mucosal to serosal (M to S) direction (Panels A and B) and the serosal to mucosal (S to M) direction (Panels C and D) across isolated short circuited segments of cecum taken from WT and DRA KO mice. A mixture of forskolin (FSK) and IBMX (to a final concentration of 0.01 and 0.1 mM respectively) was applied after 45 minutes. Corresponding changes in electrophysiological parameters, I_{sc} and G_T in WT and DRA KO tissues are shown in Panels E and F. Each data point represents the mean \pm SD from $n = 6$ (WT) and $n = 7$ (DRA-KO) tissues for measurements in the M to S direction, and $n = 10$ (WT) and $n = 7$ (DRA-KO) tissues in the S to M direction. Significant differences ($P < 0.05$) from the average of the control period (0 – 45 min) following the application of FSK/IBMX, indicated by *, were determined by one-way repeated measures ANOVA and multiple pair-wise comparisons to the control period (Holm-Sidak).

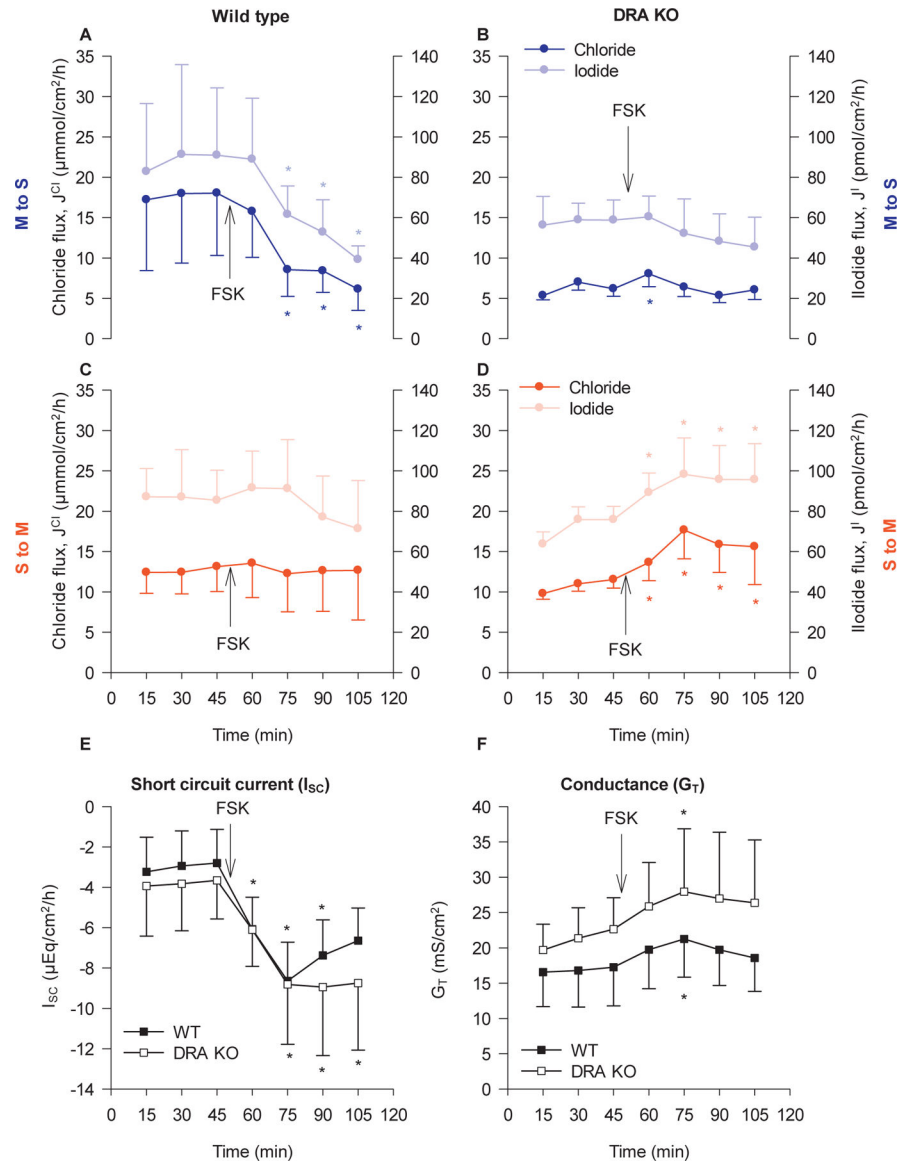


Figure 2. Chloride and iodide fluxes across the WT and DRA-KO mouse distal colon. Simultaneously measured, unidirectional J^{Cl} and J^I in the mucosal to serosal (M to S) direction (Panels A and B) and the serosal to mucosal (S to M) direction (Panels C and D) across short circuited segments of distal colon taken from WT and DRA KO mice. A mixture of forskolin (FSK) and IBMX (to a final concentration of 0.01 and 0.1 mM respectively) was applied after 45 minutes. Corresponding changes in electrophysiological parameters, I_{sc} and G_T in WT and DRA KO tissues are shown in Panels E and F. Each data point represents the mean \pm SD from $n = 10$ (WT) and $n = 7$ (DRA-KO) tissues for measurements in the M to S direction, and $n = 6$ (WT) and $n = 7$ (DRA-KO) tissues in the S to M direction. Significant differences ($P < 0.05$) from the average of the control period (0 – 45 min) following the application of FSK/IBMX, indicated by *, were determined by one-way repeated measures ANOVA and multiple pair-wise comparisons to the control period (Holm-Sidak).

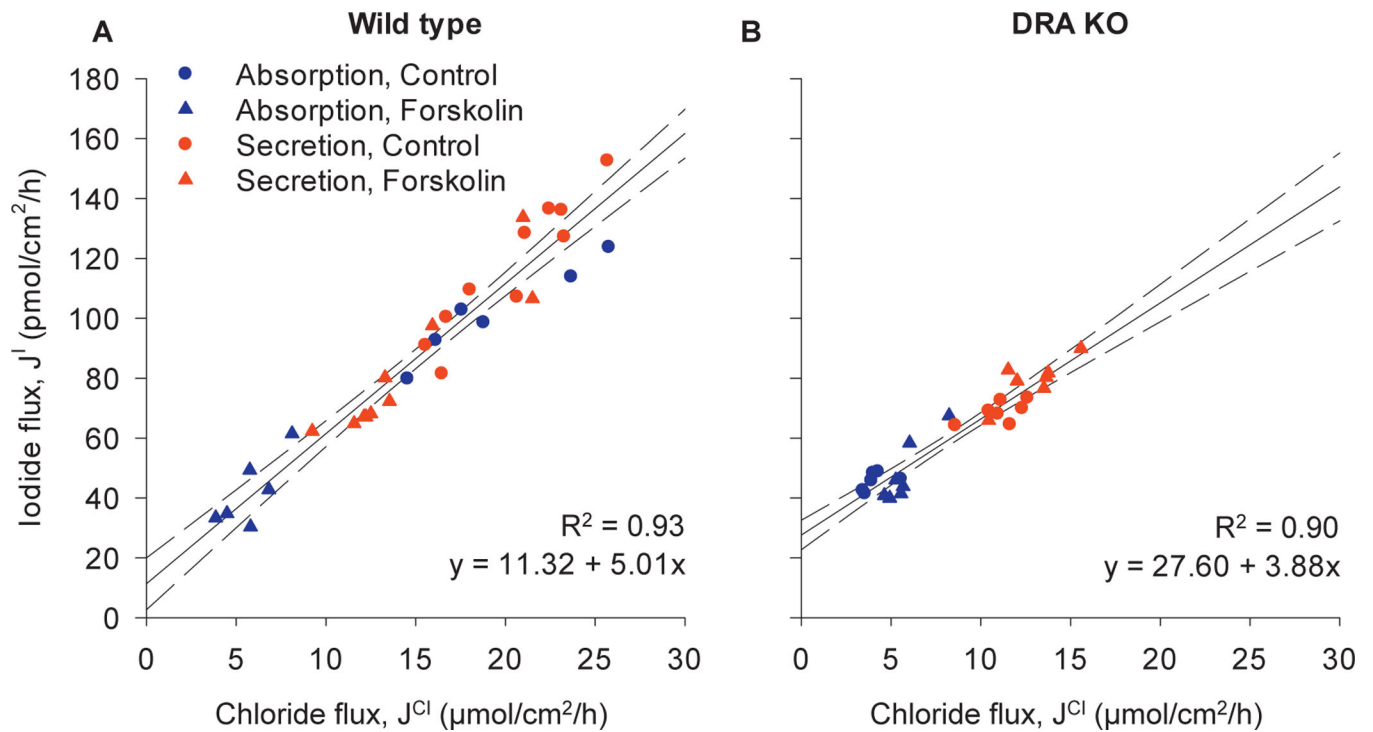


Figure 3. Relationships between J^{Cl} and J^I fluxes across the WT and DRA-KO mouse cecum. Each data point represents the average unidirectional flux for each individual tissue in either the control period, Period I, 0–45 min (circles), or the experimental period, Period II (60–105 min) following the application of FSK/IBMX (triangles). The solid line represents the predicted linear regression given by the equations in the bottom right of each panel. The intercepts and slopes were significantly different between WT and DRA KO mice ($p = 0.011$ and $p = 0.002$ for intercepts and slopes respectively). All intercepts were significantly different from zero ($p = 0.0120$ and $p < 0.0001$ for WT and DRA KO respectively). The dashed lines represent the associated 95 % confidence intervals.

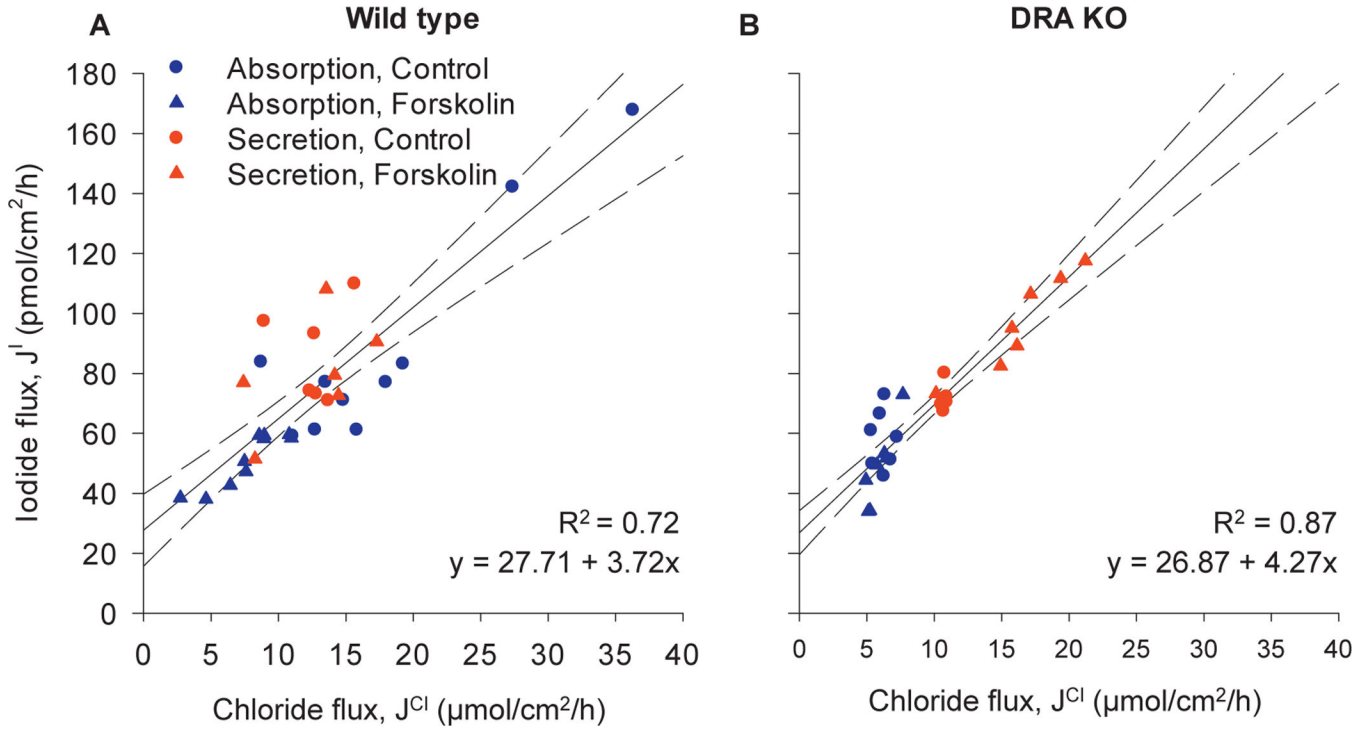


Figure 4. Relationships between J^{Cl} and J^I fluxes across the WT and DRA-KO mouse distal colon.

Each point represents the average unidirectional flux for each individual tissue in either the control period, Period I, 0–45 min (circles), or the experimental period, Period II (60–105 min) following the application of FSK/IBMX (triangles). The solid line represents the predicted linear regression given by the equations in the bottom right of each panel. The intercepts and slopes were not significantly different between WT and DRA KO mice ($p = 0.365$ and $p = 0.908$ for intercepts and slopes respectively). All intercepts were significantly different from zero ($p < 0.0001$ for both WT and DRA KO). The dashed lines represent the associated 95 % confidence intervals.